Enhanced Maximum Power Point Tracking Capability of Grid-connected Solar PV Based on Improved Bacterial Foraging Optimization

Lixiong Li*, Guanghao Zeng, Bing Wen

***Abstract*—The solar power generating system's *I-V* curve exhibits nonlinear properties. Under the condition of environmental change, the *P-V* characteristic curve of the photovoltaic array has multiple power peaks, which increases the complexity of power tracking. To address the challenge of power point tracking under sudden environmental changes, this paper introduces an enhanced maximum power point tracking strategy utilizing an improved bacterial foraging optimization algorithm. The Newton interpolation method is used to initialize the bacterial position near the global maximum power point, and the bacterial foraging algorithm has the advantage of random direction selection. When solving the optimization problem, the proposed algorithm can greatly reduce the number of iterations and improve the solution accuracy. This paper introduces a new representation approach for initialized bacterial position. The area near the maximal power point is identified using the Newton interpolation approach. The proposed method is verified through computer simulation.**

***Index Terms*—Photovoltaic, maximum power point tracking, newton interpolation calculation, bacterial foraging optimization, partial shading conditions**

I. Introduction

THE increased usage of fossil fuels in recent years has resulted in considerable environmental damage. Because of its unlimited, inexhaustible, and ecologically friendly characteristics, renewable energy has become the preferred alternative for power generation [1]. Among renewable energy sources, solar energy ranks as one of the most significant contributors to sustainable power generation. However, the low efficiency and high cost of photovoltaic power generation systems stymies the technology's continued growth. External factors like as sun irradiation and temperature have an impact on the output characteristics of solar panels. With these external influences, the maximum power point (MPP) of solar panels will change. Scholars have proposed diverse solutions for the challenges faced by MPPT controllers, including the traditional Perturb and Observe (P&O)[2] technique and the incremental conductance (IncCond)[3],[4] approach, among others. These algorithms can track power well in a stable environment, but they can't track MPP accurately in the case of mutation or slow change. Local and global peaks cannot be identified under partial shade conditions (PSC) [5],[6]. The use of the traditional MPPT algorithm in a solar power generation system in partial shadow conditions results in significant power loss, according to the literature [7]. When PSC happens, the P-V characteristics become more complex, with several peaks, affecting the controller's performance and lowering the system's output power. Different improved MPPT algorithms are proposed in [8],[9],[10] in order to measure MPP properly and increase the system reaction capabilities. These methods differ in complexity, precision, and reaction time. Despite the fact that MPP can be properly tracked, the system's dynamic response time is still poor. The swarm intelligence optimization technique can be distributed parallel search because traditional methods are difficult to deal with and lack an exact mathematical model. Because of its simple algorithm structure, ease of implementation, and quick convergence, it is often used in the field of photovoltaic power generation. In references [6] and [7], the particle swarm optimization method has been applied to the MPPT of photovoltaic power generation systems. References [10] and [11] propose enhanced versions of the artificial fish swarm and bee colony algorithms for tracking the global maximum power point (GMPP) in partial shading scenarios.

As a swarm intelligence algorithm, bacterial foraging optimization (BFO) shows great potential because of its easy realization, fast calculation speed, and MPP determination ability not affected by environmental conditions [12]. The contrast between the BFO algorithm and conventional approaches lies in the updating of the duty cycle, which is based on bacterial foraging velocity and isn't a constant. In contrast, the duty cycle is limited by the set value when using the traditional method, which affects the acquisition of the actual global maximum power point. In reference [13], the bacterial foraging optimization algorithm was used to extract the parameters of photovoltaic modules to achieve photovoltaic power conversion efficiency indirectly. Reference [14] employed an enhanced bacterial foraging algorithm to investigate parameter extraction of photovoltaic modules as a nonlinear challenge. By minimizing the mismatch error between the calculated parameters of photovoltaic modules and the nameplate parameters, the

Manuscript received October 8, 2024; revised February 15, 2025.

This work was supported by the Outstanding Youth Scientific Research Fund of Hunan Provincial Department of Education (No. 23B0744), the Hunan Natural Science Regional Joint Foundation (No. 2025JJ70378), and the Hunan Provincial Social Science Achievement Appraisal Committee Project (No. XSP24YBC180).

Lixiong Li is a lecturer of the College of Mechanical and Electrical Engineering, Hunan City University, Yiyang 413000, China. (corresponding author to provide phone: +86-18890588726; e-mail: lixiong.li@hotmail.com).

Guanghao Zeng is a postgraduate student of the College of Mechanical and Electrical Engineering, Hunan City University, Yiyang 413000, China. (e-mail: 1274881050@qq.com).

Bing Wen is a professor of the College of Information and Electronic Engineering, Hunan City University, Yiyang 413000, China. (e-mail: wenbing@hncu.edu.cn).

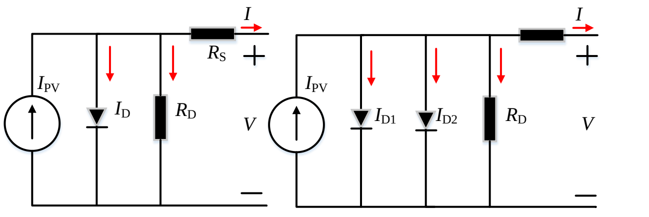

(a) (b)

Fig. 1. Photovoltaic cell.

global optimal minimum time was achieved when the global optimization was maintained. In reference [15], and improved discrete bacterial foraging optimization algorithm (DBFOA) is proposed to reduce the overall voltage imbalance of the power grid [16]. As a result, considering different network and operation parameters, the available PV capacity of the power grid is improved [17],[18],[19],[20].

Based on the characteristics of the bacterial foraging optimization algorithm, an MPPT method combining Newton Interpolation (NI) calculation method and BFO algorithm is proposed. To calculate the optimal MPP duty ratio, the Newtonian interpolation technique is applied. According to the calculated optimal duty cycle, combined with the global search feature of BFO, the global maximum power point can be dynamically tracked under the condition of sudden environmental change or gradual change, and the output power fluctuation time can be shortened to improve the system response capability.

II. Mathematical Model of Photovoltaic Power Generation System

Of the various modeling approaches for photovoltaic modules, the single-diode five-parameter model is the most commonly utilized, depicted in Fig. 1(a), while the dual-diode seven-parameter model is shown in Fig. 1(b).

The output current of the single-diode five-parameter model, as illustrated in Fig. 1(a), is

$$I = I_{\mathrm{PV}} - I_{\mathrm{D}} - I_{\mathrm{R}} \tag{1}$$

In Equation (1), the diode current can be expressed as

$$I_{\mathrm{D}} = I_0[\exp(\frac{U+IR_s}{n_s V_t}) - 1] \tag{2}$$

In formula (2), I_0 is diode reverse saturation current, V_t is the thermal voltage is determined using Equation (3)

$$V_t = \frac{ak_b T}{e} \tag{3}$$

In formula (3), k_b denotes the Boltzmann constant (1.38×10^{-23}J/K), T is the temperature of the photovoltaic module (K), and e is an electron charge. The value of I_R is obtained according to Kirchhoff's law.

$$I_{\mathrm{R}} = \frac{U+IR_s}{R_{\mathrm{D}}} \tag{4}$$

Combining Equation (1), Equation (2), and Equation (4), the output current of the single-diode five-parameter model is derived from the model

$$I = I_{\mathrm{PV}} - I_0[\exp(\frac{U+IR_s}{n_s V_t}) - 1] - \frac{U+IR_s}{R_{\mathrm{D}}} \tag{5}$$

When the solar irradiance G and the ambient temperature T change, the output current is shown in (6)

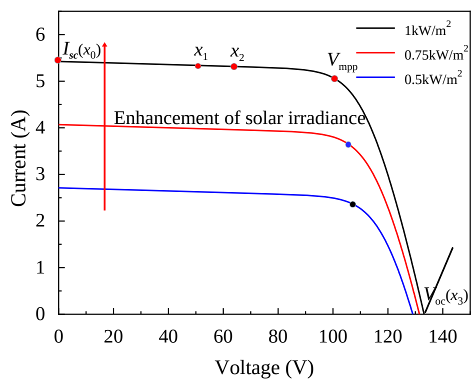

Fig. 2. I -V Characteristic of a photovoltaic cell.

$$\begin{aligned} I = {} & I_{\mathrm{PV}}(G,T) - \frac{U+IR_s(G,T)}{R_{\mathrm{D}}(G,T)} - \\ & I_0(G,T)[\exp(\frac{U+IR_s(G,T)}{n_s V_t(G,T)}) - 1] \end{aligned} \tag{6}$$

Under varying solar irradiance G and temperature T, the open-circuit voltage and short circuit current are, respectively

$$\begin{aligned} U_{\mathrm{oc}} = {} & R_{\mathrm{D}}(G,T)\{I_{\mathrm{PV}}(G,T) - \\ & I_0(G,T)[\exp(\frac{U+IR_s(G,T)}{n_s V_t(G,T)}) - 1]\} \end{aligned} \tag{7}$$

$$\begin{aligned} I_{\mathrm{sc}} = {} & \frac{R_{\mathrm{D}}(G,T)}{R_s(G,T)+R_{\mathrm{D}}(G,T)}\{I_{\mathrm{PV}}(G,T) - \\ & I_0(G,T)[\exp(\frac{U+IR_s(G,T)}{n_s V_t(G,T)}) - 1]\} \end{aligned} \tag{8}$$

Similarly, the current at the PV system MPP under varying solar irradiance G and temperature T can be calculated as

$$I_{\mathrm{MPP}} = \left(\begin{aligned} & I_{\mathrm{PV}}(G,T) - I_0(G,T) \times \\ & \exp(\frac{V_{\mathrm{MPP}}(G,T) + I_{\mathrm{MPP}} R_{\mathrm{S}}(G,T)}{n_s V_t(G,T)}) \\ & - \frac{V_{\mathrm{MPP}}(G,T) + I_{\mathrm{MPP}} R_{\mathrm{S}}(G,T)}{R_{\mathrm{P}}(G,T)} \end{aligned} \right) \tag{9}$$

The power at the maximum power point can be expressed as

$$P_{\mathrm{MPP}}(G,T) = V_{\mathrm{MPP}}(G,T) \times I_{\mathrm{MPP}}(G,T) \tag{10}$$

III. NI-BFOA Algorithm Controller Design

A. *MPPT algorithm based on numerical computing*

To rapidly locate the maximum power point and address the speed, stability, and accuracy limitations of traditional MPPT algorithms, this paper proposes a controller combining Newton interpolation (NI) and the BFO method. Initially, a constant voltage (CV) approximation is used to estimate the voltage value (V_{MPP}) of the I-V characteristics of photovoltaic modules. The CV algorithm, a simple yet effective MPPT controller, enables a quick response by assuming that the VMPP values under different irradiation levels are roughly consistent, as depicted in Fig. 2.

The calculation method is as follows: Firstly, the voltage value $V(k)$ at the current moment is obtained. Then, by using the voltage value $V(k-1)$ stored at the end of the previous cycle, four points are selected from the I–V characteristic curve of the PV characteristic curve. Then, the Newton interpolation method calculates the duty cycle d_{MPP} corresponding to the voltage (V_{MPP}) at the maximum power point. Interpolation nodes x_1 and x_2 represent voltage values corresponding to V_1 and V_2 of two sampling points. However, x_0 represents the corresponding voltage value V_0 under the short-circuit current state and equals zero. x_3 represents the corresponding voltage value of the PV module in the open-circuit state. N_1 and N_2 represent duty cycles d_1 and d_2 corresponding to voltage V_1 and V_2 at interpolation nodes x_1 and x_2. N_0 and N_3 represent the duty cycles dI_{sc} = 1 and dV_{oc} = 0, corresponding to the short-circuit current I_{sc} and the open-circuit voltage V_{oc}. As long as V_0, V_1, V_2 and V_{oc} are obtained, the duty cycle d_{MPP} corresponding to the voltage V_{MPP} at the maximum power point can be calculated by the Newton interpolation method. In Equation (11), the Newton interpolation calculation formula of d_{MPP} corresponding to V_{MPP} is given.

$$\begin{aligned} N_n(x) &= f(x_0) + f[x_0,x_1](x-x_0) + \cdots \\ &+ f[x_0,\cdots,x_n](x-x_0)(x-x_1)\cdots(x-x_{n-1}) \end{aligned} \tag{11}$$

Calculation of $N_n(x)$ by Qin Jiushao Method

$$\begin{aligned} & N_n(x) = f(x_0) + f[x_0,x_1](x-x_0) + \cdots \\ & + f[x_0,\cdots,x_n](x-x_0)(x-x_1)\cdots(x-x_{n-1}) \\ & = f(x_0) + (x-x_0)(f[x_0,x_1] + \\ & (x-x_1)(f[x_0,x_1] + \cdots + (x-x_{n-2})(f[x_0,\cdots,x_{n-2}] \\ & +(x-x_{n-1})f[x_0,\cdots,x_n])\cdots)) \end{aligned} \tag{12}$$

In formulas (11) and (12), x denotes the voltage V_{MPP} at the maximum power point, so the duty cycle d_{MPP} corresponding to V_{MPP} is calculated.

B. Bacterial foraging optimization algorithm (BFOA)

The Bacterial Foraging Optimization Algorithm (BFOA) has gained significant popularity as a distributed optimization and control algorithm for global optimization. Introduced by K. M. Passino in 2002, BFOA draws inspiration from the foraging behavior of E. coli bacteria. It is particularly effective for tackling optimization problems that are challenging for conventional methods and lack precise mathematical models [10]. BFOA optimization process is divided into four stages: chemotaxis, clustering, reproduction, elimination, and diffusion.

In the chemotaxis stage, bacteria can move or change their movement direction in a predetermined order to improve their fitness. Flip when fitness is no longer improved before and after swimming, and then change the direction of swimming randomly, e. g. (13)

$$\theta^i(j+1,k,l) = \theta^i(j+1,k,l) + C(i)\varphi(j) \tag{13}$$

In formula (13), j is the number of chemotaxes; k is the reproduction number; l is the Number of migrations; $\theta^i(j,k,l)$ is the position of individual i after j chemotaxis, k reproduction, and l migration; $C(i)$ Step length for individual i; $\varphi(j)$ is the direction of the individual i random flip.

For any bacterial individual i, the chemotactic step size formula is as follows

$$\theta^i C(i) = \gamma_1\left(\theta^{i_{best}} - \theta^i\right) + \gamma_2\left(\theta^{G_{best}} - \theta^i\right) \tag{14}$$

In formula (14), γ_1 and γ_2 are random numbers in [0,1]; $\theta^{i_{best}}$ is the optimal location of the first bacterial individual, and $\theta^{G_{best}}$ is the optimal global location of the bacterial population. In the breeding stage, the individuals are sorted according to their fitness, and the individuals with good fitness are selected for reproduction. In the elimination and diffusion stages, the diversity of bacterial populations decreases after reproduction. To help the algorithm jump out of the optimal local value (P_{best}), each bacterium generates a random number between [0,1] when the maximum reproduction number reaches. Suppose the generated random number is less than the migration probability P_{ed}, the individual points to a new position. Otherwise, the individual is not migrated and continues to search in the original position.

C. Design of BFOA for Newton interpolation (NI-BFOA)

The traditional technique uses disturbance observation power to track the MPP of PV, which leads to long calculation time and low accuracy. Based on the voltage corresponding to the maximum power point, the Newton interpolation method is used to calculate the value of d_{MPP} (duty ratio of MPP) to determine the optimal position of bacteria. So, the optimization process can be started from the initial value close to MPP.

$$d_i^j = [d_1, d_2, d_3, \cdots, d_n] \tag{15}$$

In formula (15), n is the number of bacteria, and j is the number of iterations.

The duty cycles d_1, d_2, and d_3 are initially fed into the Cùk converter. In the first iteration, these duty cycles serve as the local optimal value (P_{best}), while the global optimal value (G_{best}) is determined by the fitness value closer to the MPP. Subsequently, the duty cycles' speed and position are updated accordingly. During this process, when bacterial foraging optimization is applied, a small perturbation is introduced to the duty cycle in the next iteration. This update occurs by comparing the current fitness value with the previous one, influencing the duty cycle's adjustment in subsequent iterations. Since d_2 is the estimated value calculated by Equation (14), d_1 and d_3 can determine the upper and lower boundaries by adding and subtracting a threshold Δd for d_2. Redefining a set of duty cycles

$$d_{i*} = [d_2 - \Delta d, d_2, d_2 + \Delta d] \tag{16}$$

Continue this process by iteratively updating the duty cycle, eventually tracking the global MPP. As shown in Fig. 3, the full sequence of steps for the algorithm is presented.

IV. Algorithm Simulation Verification

A. Simulation model and parameter setting

To validate the performance and response characteristics of the proposed NI-BFOA algorithm, the system depicted in Fig. 4 is simulated using MATLAB/Simulink. Parameters for the NI-BFOA algorithm are configured as outlined in Table I. The solar module utilized is the SunPower SPR-305-WHT, with its specifications and equivalent circuit parameters detailed in Table II.

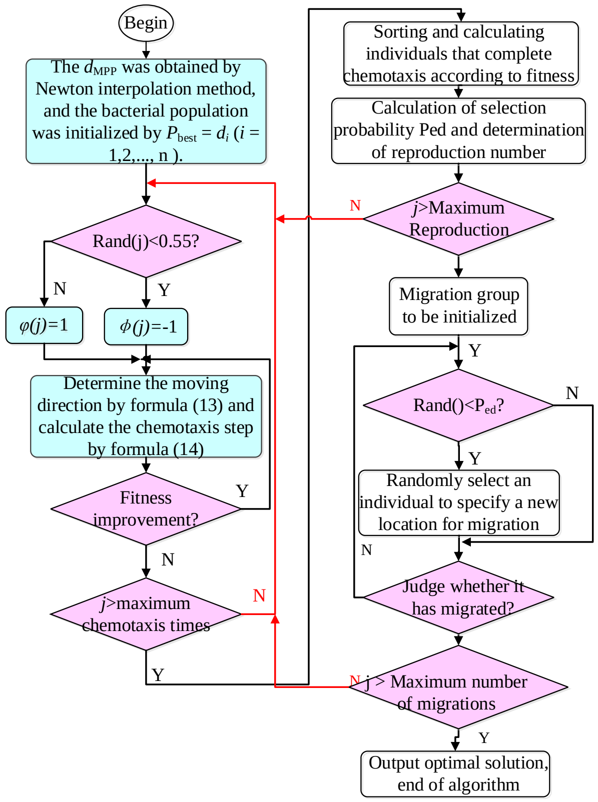

Fig.3. Flow chart of NI-BFOA.

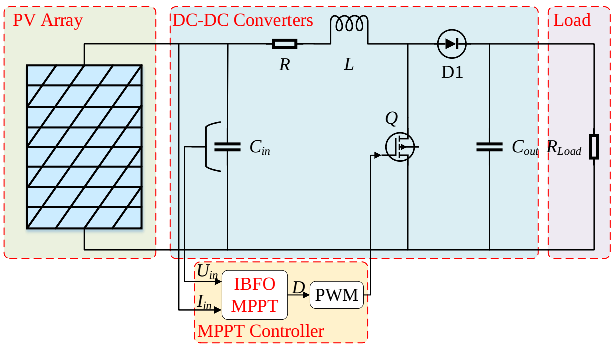

Fig. 4. Simulink model of the PV System.

TABLE I
INITIALIZATION PARAMETERS

SYMBOL	PARAMETER	VALUE
S	Total number of groups	200
N_s	Fixed step length	0.5
N_c	Number of chemotaxis iterations	5
N_{re}	Reproductive time	10
N_{ed}	Maximum transfer number	10
P_{ed}	Migration probability	0.1
C(i)	Roll-over step length	0.01
T_f	Sampling period	5μs

TABLE II
PV MODULE PARAMETERS

SYMBOL	PARAMETER	VALUE
N_{ser}	Number of serial modules	5
N_{par}	Number of parallel modules	66
N	Number of units per module	96
V_{oc}	Open circuit voltage of each module	64.2V
I_{sc}	Short-circuit current of each module	5.96V
V_{mp}	Maximum power point voltage per module	54.7V
I_{mp}	Maximum power point current per module	5.58A

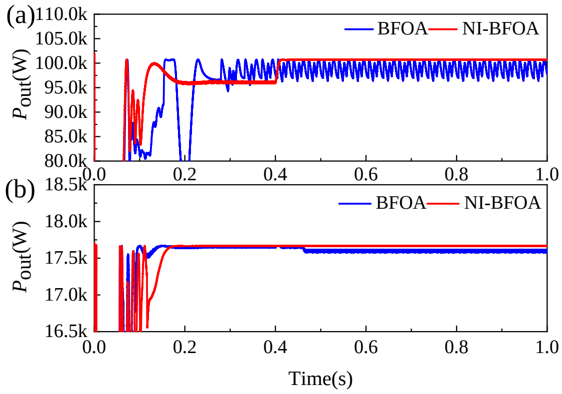

Fig. 5. Output power of photovoltaic modules in steady state. (a) G=1000 W/m^2, T=25 °C (b) G=200 W/m^2, T=25 °C

B. Photovoltaic output power in steady-state

Under steady-state conditions of ambient temperature T = 25°C, solar irradiance G = 1000 W/m^2 and G = 200 W/m^2, the proposed system is simulated by MATLAB/Simulink.

Fig. 5 (a) shows that the output power of the NI-BFOA algorithm is close to 100 kW, as can be shown. Traditional BFOA algorithm output power swings around 98 kW, and the amplitude of the fluctuation is high. Using solar irradiance G = 200 W/m^2 and a temperature of T=25°C, the output power of photovoltaic modules can be seen in Fig. 5(b). There is a 17.7kW output from the NI-BFOA algorithm, and the convergence speed is extremely fast and consistent. The classic BFOA algorithm's photovoltaic output power is 17.5 kW under the identical conditions. The output power dropped abruptly around 0.45 s.

C. A dynamic environment's effect on PV power output

Fig. 6 (a) shows the change in output power and its dynamic response when the solar radiation received by photovoltaic modules changes from 300 W/m^2 to 500 W/m^2 at a constant temperature of T = 25 °C. Solar irradiation drops from 1000W/m^2 to 500W/m^2 as seen in Fig. 6 (b). As shown in Figures 6 (a) and (b), NI-BFOA responds more quickly to changes in solar irradiance and has a higher output power than standard BFOA. As demonstrated in Fig. 6, the dynamic responses of the system output power at various ambient temperatures of zero, 25 degrees Celsius, 75 degrees Celsius, and 50 degrees Celsius are illustrated (c). For both dynamic and steady state responses, the NI-BFOA algorithm outperforms the classic BFOA algorithm.

The NI-BFOA algorithm is compared to the regular BFOA in a simulation in order to validate its efficiency under partial shadow situations. The simulation model of the photovoltaic array is composed of four photovoltaic modules in series. The solar irradiances of each module are G_1, G_2, G_3, and G_4, respectively, and the initial state is 1 000 W/m^2. At the time t = 1s, G_1 keeps the solar irradiance unchanged, and G_2, G_3, and G_4 decrease to 800 W/m^2, 500 W/m^2, and 300 W/m^2, respectively. At this time, the output power of the PV array using the NI-BFOA algorithm fluctuates around 1335 W, while the output power of the PV array using the traditional BFOA algorithm is 1181 W, as shown in Fig. 7.

D. Under dynamic environment, photovoltaic output voltage

Different shadow situations are used to test the output

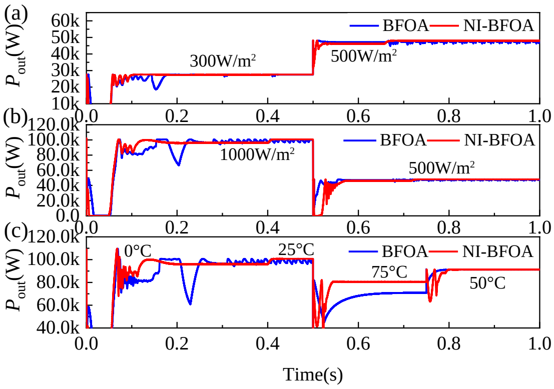

Fig. 6. Output power of photovoltaic modules in a dynamic environment. (a) G sudden increase, T = 25 °C, (b) G sudden decrease, T = 25 °C, (c) G = 1 000 W/m^2, T change.

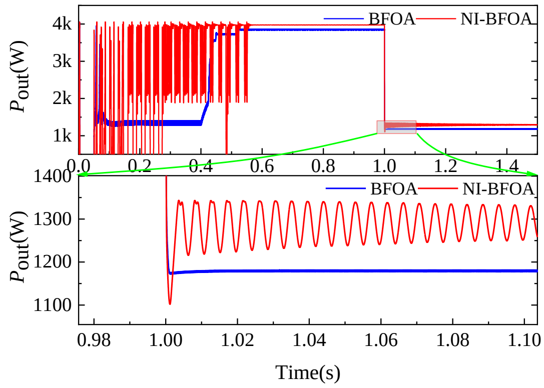

Fig. 7. Output power of photovoltaic modules under partial shading conditions.

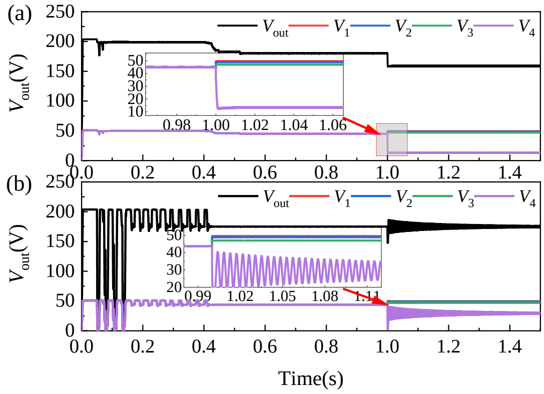

Fig. 8. System voltages tested under partial shading conditions; (a) Traditional BFOA, (b) NI-BFOA.

voltage of the solar power generation system using the BFOA algorithm and NI-BFOA algorithm. Fig. 8 (a) and Fig. 8 (b) display the test findings. The solar irradiance received by photovoltaic panels are: G_1 = 1 000 W/m^2, G_2 = 800 W/m^2, G_3 = 500 W/m^2, G_4 = 300 W/m^2. In Fig. 8 (a) and Fig. 8 (b), V_{out} represents the total output voltage, V_1 represents the output voltage of the photovoltaic module at the irradiance (G_1) of 1000 W/m^2, V_2 represents the output voltage of the photovoltaic module at the irradiance (G_2) of 800 W/m^2, V_3 represents the output voltage of the photovoltaic module at the irradiance (G_3) of 500 W/m^2, and V_4 represents the output voltage of the photovoltaic module at the irradiance (G_4) of 300 W/m^2.With Fig. 8 (a) compared to Fig. 8 (b), the NI-BFOA algorithm's output voltage is slightly higher than that of its traditional counterpart. It is true that when G_4 is 300 W/m^2, the PV control system employing NI-BFOA algorithm's output voltage ripple is huge, but it's more than twice as high as the classic BFOA algorithm's output voltage. The output power of the former is also much greater than its counterpart.

E. Study on the dynamic process under continuous temperature change

In a photovoltaic environment, ambient temperature changes are steady and continuous. To assess the effectiveness of the NI-BFOA algorithm in dynamic settings, we compared the BFOA results under conditions of gradual warming and cooling. During our simulations, we focused on the first 5 seconds of both the heating phase in section A and the cooling phase in section B, as shown in Fig. 9, to measure their respective temperature change rates. The temperature was varied from 0 to 50 degrees, and solar irradiance was maintained at 1000W/m² to clearly demonstrate the PV power trend, as depicted in Fig. 9.

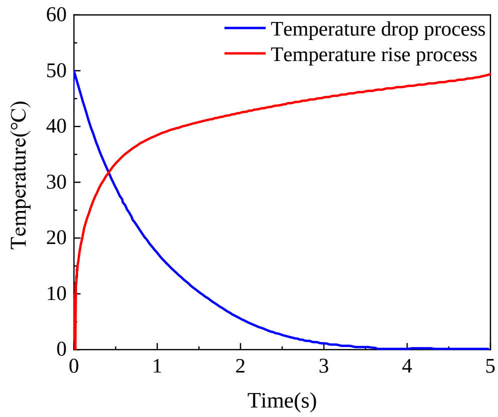

Fig. 9. Trend of ambient temperature in which the PV system is located.

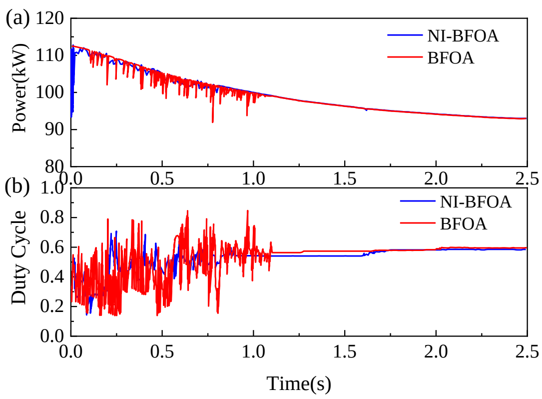

Fig. 10. Temperature rise process;(a) Power, (b) Duty cycle.

1) Temperature rise process

The NI-BFOA algorithm demonstrates the quickest search speed with minimal power fluctuation during temperature increases. Fig. 10(b) shows that within the first 0.25 seconds of initialization, the duty cycle values for BFOA and NI-BFOA almost reach the error position of 0.4. The BFOA algorithm restarts in 1.06 seconds and efficiently tracks the global maximum power point. In contrast to BFOA, NI-BFOA achieves a stable transition to MPP in 0.85 seconds, reducing the convergence time by 21.4%. During the search phase, which spans 1.08 seconds, NI-BFOA consistently tracks the MPP with slight power fluctuations.

2) Temperature drop process

Even though the ambient temperature decreases, the MPP's position remains fairly steady. Frequently restarting algorithms can cause substantial energy consumption. Fig. 11 shows that when tracking maximum power, BFOA's power varies significantly due to regular algorithm reinitialization. NI-BFOA stopped the algorithm restart in 0.214 seconds, and after a period of stable operation, it restarted and began secondary tracking at 0.73 seconds, eventually achieving a relatively stable state. The convergence times for BFOA and NI-BFOA were 1.53 and 0.82 seconds, respectively. The convergence time of NI-BFOA is 46.4% shorter than that of BFOA.

As shown in Fig. 11(a), the NI-BFOA algorithm achieves rapid convergence with minimal power oscillations. However, the convergence time of the conventional BFOA method under gradually decreasing temperature conditions is significantly longer than that of the proposed NI-BFOA method. As the photovoltaic power continues to increase, the duty cycle of the BFOA fluctuates significantly, leading to potential high power losses and fluctuations in output power.

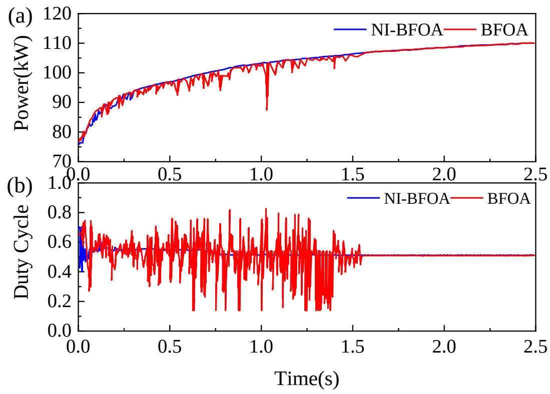

Fig. 11. Temperature drop process;(a) Power, (b) Duty cycle.

F. Experimental statistical analysis

The solar irradiance of the four photovoltaic modules was set to G_1=1000 W/m^2, G_2=800 W/m^2, G_3=500 W/m^2, G_4=300 W/m^2, and the ambient temperature was kept stable at T=25°C. The solar irradiance of the four photovoltaic modules was set to G_1=1000 W/m^2, G_2=800 W/m^2, G_3=500 W/m^2, and G_4=300 W/m^2, respectively. The NI-BFOA algorithm selects the number of populations as 20, considering the fast realization of tracking the maximum power point, so the parameter setting should not be too large, otherwise, the convergence time is too long. Therefore, two groups of experiments were set up. The number of tendentious movements in group A was 5, and the number of replications was 3. The number of tendentious movements in group B was 7, and the number of replications was 5.

The two sets of experiments were run 20 times each and the results of the algorithm execution are shown in Table III. The data from Table III clearly show that the bacterial foraging algorithm, when combined with Newton's interpolation, is capable of avoiding local optima and identifying the global maximum power point. Reducing the convergent motion and replication number parameters can speed up the convergence speed, but the maximum power point found is not stable, therefore, taking into account to satisfy the fast convergence, appropriately expanding the convergent motion and replication operation parameters can enhance the stability of the algorithm.

TABLE III
THE RESULTS OF NI-BFOA

Number of runs	Group A experiment		Group B experiment	
	Iteration times	P_{max}(W)	Iteration times	P_{max}(W)
1	11	1334.266	16	1334.49
2	12	1334.931	17	1334.592
3	13	1334.419	13	1334.421
4	13	1334.571	18	1334.095
5	12	1334.822	16	1334.493
6	11	1334.280	19	1334.310
7	13	1334.521	14	1334.799
8	17	1334.166	16	1334.737
9	15	1334.808	13	1334.814
10	16	1334.093	13	1334.942
11	15	1334.268	16	1334.685
12	15	1334.927	15	1334.031
13	14	1334.057	16	1334.445
14	13	1334.625	18	1334.913
15	12	1334.994	18	1334.142
16	15	1334.488	13	1334.771
17	17	1334.548	14	1334.913
18	12	1334.032	13	1334.863
19	14	1334.944	16	1334.305
20	15	1334.136	17	1334.878
average value	13.75	1334.494	15.55	1334.637

V. CONCLUSION

It is proposed in this study that a system for efficiently internalizing the bacterial position around MPP be used to avoid repeated searching and a situation in which the active searching region of bacterial foraging is too limited. The simulation outcomes indicate that the NI-BFOA algorithm, which integrates bacterial foraging with Newton interpolation, outperforms other techniques in terms of responsiveness and tracking efficiency. It is capable of swiftly and autonomously relocating to the optimal or a vicinity of the optimal position in response to altering environmental conditions. This efficiency minimizes the time spent by the algorithm in unproductive regions and overcomes the limitations imposed by multiple local optima. Consequently, it can precisely identify the maximum power point within the prevailing environment. Additionally, once the maximum power point is pinpointed, the algorithm effectively reduces the steady-state oscillation associated with it.

REFERENCES

[1] Subudhi B, Pradhan R. A comparative study on maximum power point tracking techniques for photovoltaic power systems[J]. *IEEE transactions on Sustainable Energy*, vol.4, no.1, pp 89-98, 2012.

[2] Chikh A, Chandra A. An optimal maximum power point tracking algorithm for PV systems with climatic parameters estimation[J]. *IEEE Transactions on Sustainable Energy*, vol.6, no.2, pp 644-652, 2015.

[3] Tey K S, Mekhilef S. Modified incremental conductance algorithm for photovoltaic system under partial shading conditions and load variation[J]. *IEEE Transactions on Industrial Electronics*, vol.61, no.10, pp 5384-5392, 2014.

[4] Elgendy M A, Zahawi B, Atkinson D J. Operating characteristics of the P&O algorithm at high perturbation frequencies for standalone PV

systems[J]. *IEEE Transactions on Energy Conversion*, vol.30, no.1, pp 189-198, 2015.

[5] Ahmed J, Salam Z. An enhanced adaptive P&O MPPT for fast and efficient tracking under varying environmental conditions[J]. *IEEE Transactions on Sustainable Energy*, vol.9, no.3, pp 1487-1496, 2018.

[6] Renaudineau H, Donatantonio F, Fontchastagner J, et al. A PSO-based global MPPT technique fordistributed PV power generation[J]. *IEEE Transactions on Industrial Electronics*, vol.62, no.2, pp1047-1058, 2015.

[7] Subudhi B, Pradhan R. Bacterial foraging optimization approach to parameter extraction of a photovoltaic module[J]. *IEEE Transactions on Sustainable Energy*, 2017, vol.9, no.1, pp 381-389, 2017.

[8] Dagal I, Akın B, Akboy E. A novel hybrid series salp particle Swarm optimization (SSPSO) for standalone battery charging applications[J]. *Ain Shams Engineering Journal*, 2022, vol.13, no.5, pp 101747, 2022.

[9] Mao M, Duan Q, Duan P, et al. Comprehensive improvement of artificial fish swarm algorithm for global MPPT in PV system under partial shading conditions[J]. *Transactions of the Institute of Measurement and Control*, vol.40, no.7, pp 2178-2199, 2018.

[10] Subudhi B, Pradhan R. Bacterial foraging optimization approach to parameter extraction of a photovoltaic module[J]. *IEEE Transactions on Sustainable Energy*, vol.9, no.1, pp 381-389, 2017.

[11] Awadallah M A. Variations of the bacterial foraging algorithm for the extraction of PV module parameters from nameplate data[J]. *Energy Conversion & Management*, vol.113, pp 312-320, 2016.

[12] Bandara W G C, Godaliyadda G, Ekanayake M P B, et al. Coordinated photovoltaic re-phasing: A novel method to maximize renewable energy integration in low voltage networks by mitigating network unbalances[J]. *Applied Energy*, vol.280, pp 116022, 2020.

[13] Li Lixiong, Yang Tongguang, Yuan Yueyang, Cai Zhenhua. Maximum power point tracking algorithm of a photovoltaic power generation system based on an improved finite set model predictive control strategy[J]. *Power System Protection and Control*, vol.49, no.17, pp 28-37, 2021.

[14] Xiong G, Zhang J, Shi D, et al. Parameter extraction of solar photovoltaic models using an improved whale optimization algorithm[J]. *Energy conversion and management*, vol.174, pp 388-405, 2018.

[15] Alanis A Y, Arana-Daniel N, Lopez-Franco C. Bacterial foraging optimization algorithm to improve a discrete-time neural second order sliding mode controller[J]. *Applied Mathematics and Computation*, vol.271, pp 43-51, 2015.

[16] Wang B, Sun Q, Wang R, et al. Mitigation of interharmonics in PV systems: A cyber-physical co-regulation based maximum power point tracking algorithm[J]. *International Transactions on Electrical Energy Systems*, vol.31, no.12, pp e13249, 2021.

[17] Li J, Wu Y, Ma S, et al. Analysis of photovoltaic array maximum power point tracking under uniform environment and partial shading condition: A review[J]. *Energy Reports*, vol.8, pp 13235-13252,2022.

[18] Dagal I, Akın B, Akboy E. A novel hybrid series salp particle Swarm optimization (SSPSO) for standalone battery charging applications[J]. *Ain Shams Engineering Journal*, vol.13, no.5, pp 101747, 2022.

[19] Li L, Yang T, Yuan Y, et al. A novel power balance control scheme for cascaded H-bridge multilevel converters with battery energy storage[J]. *International Journal of Electrical Power & Energy Systems*, vol. 148, pp 108977,2023.

[20] Ragb O, Bakr H. A new technique for estimation of photovoltaic system and tracking power peaks of PV array under partial shading[J]. *Energy*, vol.268, pp 126680, 2023.